Examining the conformational dynamics of macromolecules with time-resolved synchrotron X-ray 'footprinting'

Mark R Chance*[1,2,3] , Bianca Sclavi[1,3], Sarah A Woodson[4] and Michael Brenowitz[2,3]

Addresses: [1]Department of Physiology and Biophysics, Albert Einstein College of Medicine of Yeshiva University, 1300 Morris Park Ave, Bronx, NY 10461, USA, [2]Department of Biochemistry Albert Einstein College of Medicine of Yeshiva University, 1300 Morris Park Ave, Bronx, NY 10461, USA, [3]The Center for Synchrotron Biosciences, Albert Einstein College of Medicine of Yeshiva University, 1300 Morris Park Ave., Bronx, NY 10461, USA and [4]Department of Chemistry and Biochemistry, University of Maryland, College Park MD, 20742, USA.

*Corresponding author.
E-mail: mrc@aecom.yu.edu

Structure 15 July 1997, 5:865–869
http://biomednet.com/elecref/0969212600500865

Achieving an understanding of the conformational dynamics of macromolecules during processes as diverse as ligand binding, folding and catalysis is a challenging and important step towards the goal of providing detailed molecular descriptions of biological systems. An important route towards this goal is the development of methods capable of monitoring these processes both with high structural resolution and in real time. Historically, many of the methods developed to examine conformational changes as a function of solvent accessibility were based upon modification or cleavage reactions, such as iodination or limited proteolysis. The development of a nuclease protection assay ('footprinting') was a breakthrough in the analysis of protein–DNA interactions. The original implementation of this approach [1] involved limited digestion of DNA with DNase I, such that each position along the phosphodiester backbone of the DNA was sampled by the nuclease with equal probability. Following digestion, the nuclease reaction products were separated by gel electrophoresis capable of resolving DNA fragments differing in size by one nucleotide to provide qualitative portraits ('footprints') of sequence-specific protein–DNA interactions. Footprinting techniques have been successfully extended through the application of a variety of enzymatic and chemical nucleases [2], including the hydroxyl radical (•OH) generated by the Fenton–Haber–Weiss reaction using Fe-EDTA as a catalyst [3].

Quantitative time-resolved protocols have been developed for DNase I footprinting experiments for the determination of thermodynamic and kinetic constants describing protein–DNA interactions [4–6]. Technical considerations limit the time resolution of the DNase I kinetics method to timescales of the order of tens of milliseconds, however. Also, enzymatic nucleases such as DNase I are frequently insensitive to structural changes that occur within protein-binding sites. In contrast, a cleavage reagent such as the hydroxyl radical can potentially provide single-base structural resolution. The two reagents commonly used to generate •OH for footprinting experiments, Fe-EDTA and peroxonitrite, however, cannot be used for reaction timescales of less than minutes [7,8] and seconds [9], respectively.

An ideal method for the kinetic analysis of conformational dynamics, and also what we call structural kinetics, would provide high structural resolution on timescales shorter than the conformational transition, as well as monitoring multiple processes simultaneously and making parsimonious use of precious samples. Unfortunately, these goals are often incompatible, as seen from the following examples. Fluorescence spectroscopy has some ideal properties—it has enviable time resolution, requires small sample quantities, provides solution phase information and can probe interactions at both the solvent interface and interior of a macromolecule. But the fluorescent probes must be separately placed to probe different regions of the macromolecule, the necessary chromophores may be difficult or impossible to insert in the macromolecule of interest and may be limited by the overlap of the fluorescence spectra. Nuclear magnetic resonance (NMR) spectroscopy has enviable structural resolution, but it requires milligram sample quantities, is difficult or impossible to apply to large macromolecules and kinetic structural analysis by this method is a challenge. Inventive approaches to NMR, such as deuterium exchange quench studies of protein folding [10], have yielded insight into conformational dynamics of macromolecules with high structural resolution, however.

Thus, there is clearly room for the development of new approaches to understanding the problems of folding and macromolecular interactions. We are developing a time-resolved footprinting approach using •OH as the probe, with the goal of simultaneously fulfilling as many of the criteria outlined above as possible. In this article, we review the application of this approach to the study of RNA folding. Considering the enthusiasm and attention given to the study of protein folding, the biological importance of RNA folding is quite clear. Mutations that cause aberrant folding of RNAs can clearly lead to diseases. In addition, changes in RNA conformation are probably important as regulatory switches in gene expression and development. The method of time-resolved synchrotron X-ray footprinting, which can provide high structural resolution,

Figure 1

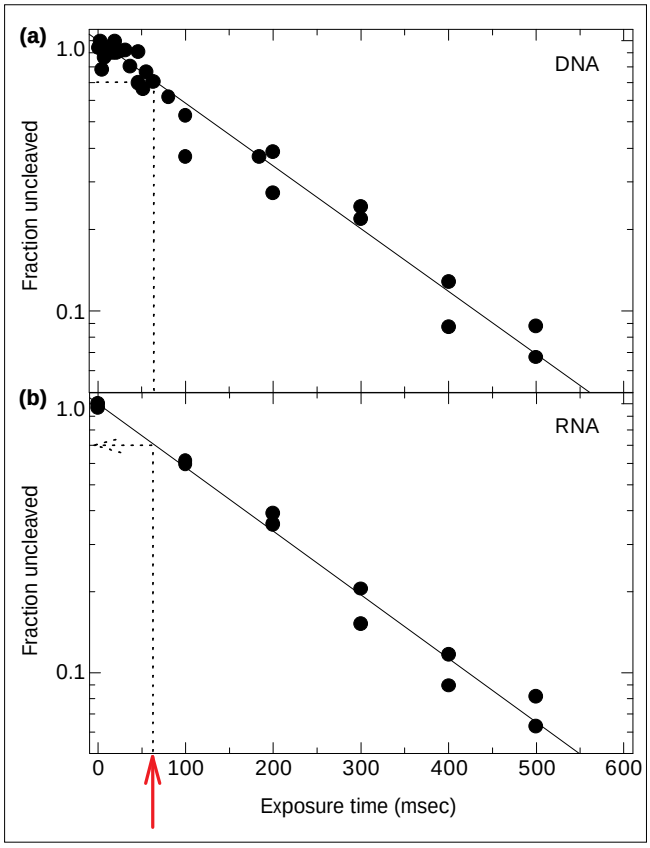

Dose-response curves relating the amount of DNA and RNA that remains uncleaved to the time of synchrotron X-ray beam exposure. (a) The DNA used was an *Eco*R1 / *Hind* III DNA restriction fragment of 185 bp, excised from the plasmid pDW001. This fragment was 3′ end-labeled at the *Hind* III restriction site with a single ^{32}P-labeled nucleotide. (b) The RNA sample was the *Tetrahymena* L-21 ribozyme, which was 5′ end-radiolabeled by kinase and γ-[^{32}P]-ATP. Exposure of the ^{32}P-DNA and ^{32}P-RNA samples to the X-ray beam was accomplished using a calibrated remote-controlled shutter. Exposed samples were analyzed by gel electrophoresis and the intensity of the uncut band on the gel is plotted in the figure against exposure time. The data sets shown represent multiple independent determinations. The dotted lines indicate the time of X-ray beam exposure required to nick ~30% of the nucleic acids, as required for conducting footprinting experiments.

sensitivity to solvent accessibility, parsimonious use of RNA and millisecond time resolution, is ideally suited to examining questions relating to RNA structural kinetics and conformational dynamics. We also discuss the application of this approach to DNA conformational dynamics, protein–nucleic acid interactions and the footprinting of proteins.

Time-resolved synchrotron X-ray footprinting

Nucleic acid cleavage by •OH is predominantly dependent upon the solvent accessibility of the phosphodiester backbone and is relatively insensitive to base sequence or to whether the nucleic acid is single or double stranded [11]. We use a radiolysis method to generate hydroxyl radicals according to equation 1 [12].

$$H_2O \xrightarrow{h\nu} H_2O^+ + e^-_{dry} \xrightarrow{H_2O} H_3O^+ + \bullet OH + e^-_{aq} \quad (1)$$

Irradiation of aqueous solutions with various forms of radiation, including γ-rays, β-particles and fast neutrons, has been successfully used to obtain structural data for sequence-specific protein–DNA complexes comparable to those obtained with chemically generated •OH footprinting methods [13–15]. The use of radiolytic sources with low total flux required sample exposure times of the order of hours, however. In contrast, an unfocused 'white beam' bending magnet beamline at the National Synchrotron Light Source (NSLS) delivers ~10^{15} photons sec^{-1} of a continuous spectrum of 1–30 keV X-rays, in a beam characterized by relatively little divergence. Figure 1 shows that the flux provided by NSLS beamline X-19C results in DNA and RNA footprinting with X-ray exposures of tens of milliseconds [8]. Beamline exposures as short as 10 milliseconds are now possible on the newly commissioned X-9A footprinting beamline of the Center for Synchrotron Biosciences (MRC, BS and MB unpublished data). This tremendous shortening of the footprinting timescale is obtained without the need to add chemical reagents to the solution of macromolecules and is a breakthrough in the study of the time-dependent analysis of nucleic acid structure with individual base resolution.

Synchrotron X-ray footprinting of an RNA-folding reaction

A representation of the secondary structure and predicted tertiary organization of the 388 bp L-21 Sca I *Tetrahymena thermophilia* ribozyme is shown in Figure 2; the tertiary organization shown is based on molecular modeling and biochemical studies [16,17]. The ribozyme adopts a compact structure in the presence of divalent cations; Mg^{2+} is specifically required for catalytic activity [18]. The tertiary contacts in the P4–P6 domain, containing paired regions P4, P5 and P6 (Figure 2), have been elegantly confirmed by the elucidation of the crystal structure of the domain [19]. The crystal structure has also illuminated many other aspects of the RNA molecular structure and it provides an important framework for the interpretation of the kinetic data. In addition, there is a high correlation between •OH reactivity and solvent accessibility of the ribose C4′ which is calculated from the P4–P6 crystal structure [19], demonstrating the validity of •OH footprinting as a structural probe. Nucleotides that are protected from •OH cleavage upon the addition of Mg^{2+} are interpreted as being involved in tertiary structure contacts that result in the interface being excluded from connections to the 'bulk' solvent. Thus, the increases in •OH protection that occur throughout the ribozyme as a function of time following the addition of Mg^{2+} reflect the ongoing folding process. The *Tetrahymena* ribozyme is an excellent system to use for the development

Figure 2

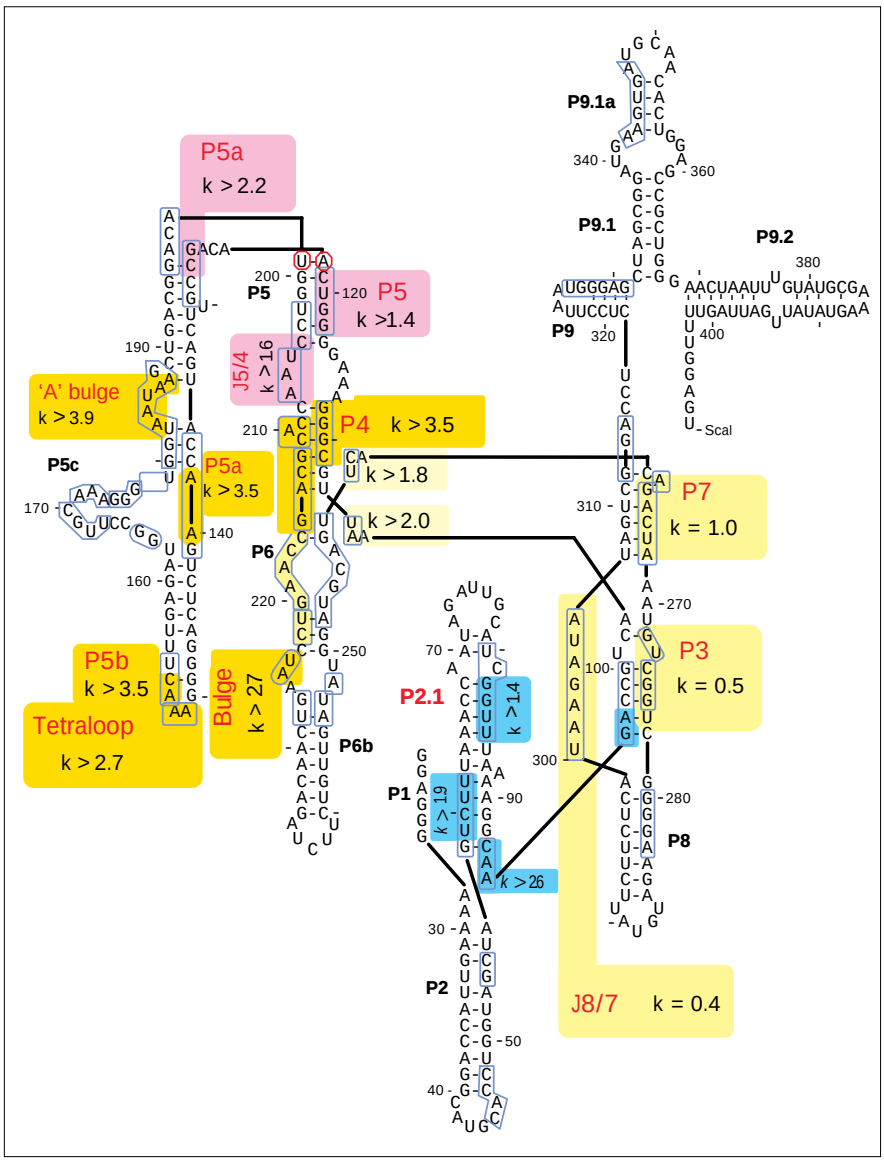

Secondary structure of the L-21 Sca I *Tetrahymena* ribozyme. Paired (P) and joining (J) regions are numbered sequentially [25]. Left, P4–P6 domain; center, P1–P2 domain; right, P3–P7 domain. The A-rich bulge (nucleotides 182–188) and GAAA tetraloop (149–154) make tertiary interactions that are essential for folding of the P4–P6 domain. The outlined bases are protected from, or become hypersensitive to, •OH cleavage upon the addition of Mg^{2+}. The values of *k* (rate constant, min^{-1}) determined for selected regions are shown in the colored boxes; boxes of the same color highlight sequences that have comparable folding rates. The rates shown for P7, P3 and J8/7 are quite accurate. Although those for the other regions are only lower limits, due to the 'dead time' of the hand mixing experiments, a comparison of the numbers provides an accurate ordering of the folding process.

of this time-resolved footprinting approach, because its complete Mg^{2+}-dependent folding occurs on a timescale of minutes allowing both manual and stopped-flow mixing methods to be successfully applied.

Figure 3 shows kinetic progress curves determined using a manual-mixing implementation of the synchrotron X-ray footprinting approach [8]. The protection of the bases within the interior of the P4–P6 domain (Figure 3b) is virtually complete within the ~30 sec dead-time of the manual-mixing method. In contrast, a complete progress curve with a rate constant (k) of 0.5 min^{-1} is determined for the P3 domain within the catalytic core (Figure 3a). The existence of multiple folding intermediates are demonstrated, with the folding of the P4–P6 domain being the first step in the reaction and the assembly of the catalytic core of the ribozyme being the slowest step. These results are consistent with data of Zarrinkar and Williamson [20], who developed an elegant oligonucleotide-hybridization–competition manual-mixing assay to monitor the folding pathway of the ribozyme.

Figure 2 summarizes the results of manual-mixing synchrotron X-ray footprinting kinetics experiments for the Mg^{2+}-dependent folding of the ribozyme [8]. The fact that the folding kinetics of regions within the interior of the P4–P6 domain (Figure 2, orange boxes) proceeds at rates faster than can be accurately measured with manual mixing, in contrast to the relatively slow rates of protection observed for the catalytic core (Figure 2, yellow boxes), is

Figure 3

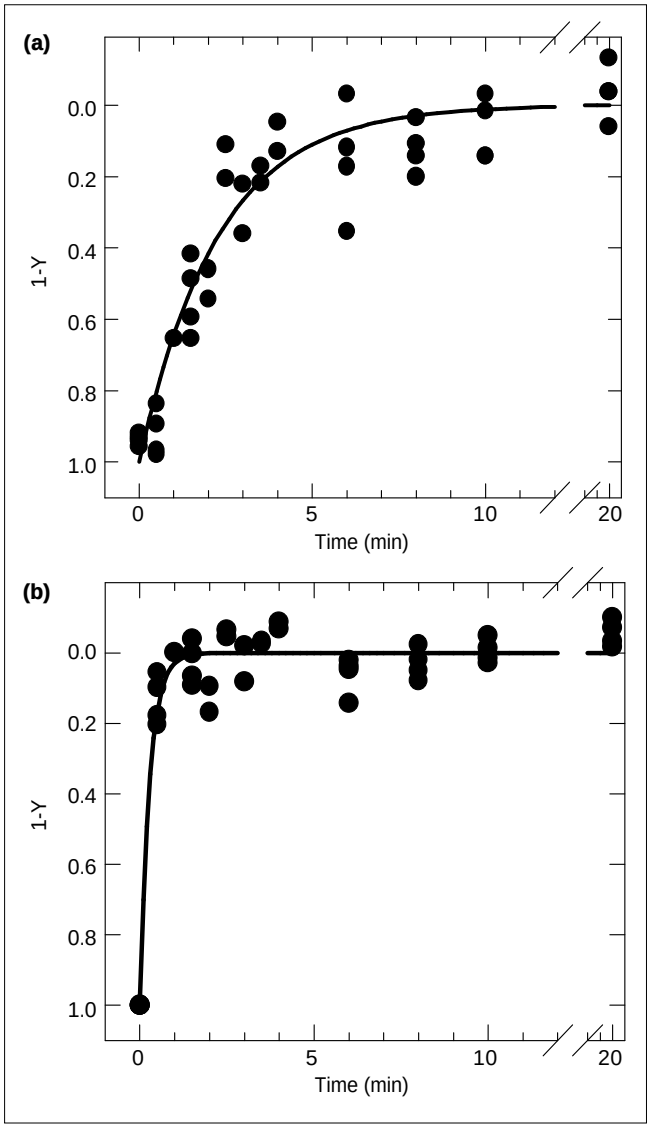

Kinetic progress curves at 10 mM $MgCl_2$ for the Mg^{2+}-dependent folding of the *Tetrahymena* ribozyme: (a) bases 272–277 (P3); (b) bases 139–140 (P5a). The *x* axis reflects time after mixing of the RNA with Mg^{2+}, the *y* axis reflects the extent of protection, where 1.0 is the extent of protection seen in unfolded RNA and 0.0 is the extent of protection seen in the equilibrium folded RNA controls; Y is equal to the fraction of RNA that is folded.

evidence that the P4–P6 domain is essentially completely folded prior to the accumulation of significant concentrations of the completely folded ribozyme. This conclusion is consistent with demonstrations that this domain can fold independently into a structure that stabilizes the ribozyme's core upon re-assembly [7,21,22].

The •OH protection kinetic data suggest a model for the folding pathway of the *Tetrahymena* ribozyme, in which the fastest step in the reaction is the folding of the P4–P6 domain [8,20]. The slower rates of protection observed for nucleotides in and adjacent to P5 (Figure 2; purple boxes) which are thought to interact with P9 [23] imply that P9 docks onto the folded P4–P6 domain. Assembly of the P3–P7 domain is thought to be stabilized by prior formation of the triple helix, which organizes the compact core of the ribozyme [20,22]. Slow protection (folding) of P3–P7 may arise from thermodynamic instability of the triple helix, or from non-native contacts that kinetically compete with native interactions.

To answer the many questions raised by the predictions made from this RNA-folding model will require the acquisition of kinetic progress curves on millisecond timescales for many regions of the RNA that are protected upon Mg^{+2} binding. For example, as the folding of the P4–P6 domain precedes that of the catalytic core, is its folding completely concerted or can individual steps be discerned? What is the largest structure of the RNA that can fold cooperatively? Also, is the folding necessarily hierarchical (e.g. do subsequent steps, if any, depend on the correct folding of P4–P6)? To what extent does misfolding impede the folding process? Although the answers to these questions are beyond the scope of this review, we have developed the methodology to directly address such detailed questions relating to the folding of this and other RNAs. A stopped-flow footprinting apparatus has been constructed and installed on NSLS beamline X–9A. The device provides millisecond mixing and exposure to the X-ray beam. Our experience with this device clearly shows the time-resolved footprinting method can follow conformational dynamics of nucleic acids (when significant changes in protection occur) on the tens of milliseconds timescale.

Conclusions and implications for future research

A new approach of synchrotron X-ray footprinting has been developed for the analysis of time-resolved structural changes and macromolecular interactions. The application of this technology to the study of the *Tetrahymena* ribozyme folding mechanism will result in the detailed elucidation of its folding pathway, covering four orders of magnitude in time (10 milliseconds to minutes) with potential single nucleotide resolution. This approach is also applicable to the folding of a large number of biologically important RNA molecules. The conduct of folding experiments as a function of thermodynamically relevant variables and their analysis by X-ray footprinting will also provide information about the chemical forces driving the reaction, not just for the entire molecule but for numerous individual regions of the molecule. These analyses, especially where 3-D structural data are available, will provide unprecedented insight into the chemical and structural features that dictate particular folding rates. We also suspect that this method could be applied to complex macromolecular assemblies, or used for studies *in vivo*. Lastly, the extension of this method to

protein footprinting should be considered, as protein footprinting using Fe-EDTA-generated •OH has been successfully demonstrated [24]. As we demonstrate for nucleic acid footprinting, the timescale achievable for protein footprinting should be reduced by four or more orders of magnitude relative to the Fe-EDTA method, also bringing it into the milliseconds range. Thus, we can envision the use of the footprinting approach to probe protein folding, protein–protein interactions and nucleic acid–protein interactions from the perspective of the protein.

Acknowledgements

This work is supported by grants from the National Center for Research Resources (RR-01633, MRC) and the National Institute for General Medical Sciences (GM-52348, MRC; GM-51506, M.B. & GM-46686, S.W.) of the National Institutes of Health. The operation of the NSLS is supported by the Office of Basic Energy Sciences, Department of Energy. We also thank Mike Sullivan for assistance in this project.

References

1. Galas, D. & Schmitz, A. (1978). DNase footprinting: a simple method for the detection of protein–DNA binding specificity. *Nucl. Acids Res.* 5, 3157–3170.
2. Revzin, A. (ed.) (1993). Footprinting Techniques for Studying Nucleic Acid-Protein Complexes (A Volume of Separation, Detection, and Characterization of Biological Macromolecules), Academic Press, New York.
3. Tullius, T.D., Dombroski, B.A., Churchill, M.E. & Kam, L. (1987). Hydroxyl radical footprinting: a high resolution method for mapping protein–DNA contacts. *Methods Enzymol.* 155, 537–558.
4. Brenowitz, M., Senear, D.F., Shea, M.A. & Ackers, G.K. (1986). Quantitative DNase footprint titration: a method for studying protein–DNA interactions. *Methods Enzymol.* 130, 132–181.
5. Hsieh, M. & Brenowitz, M. (1996). Quantitative kinetics footprinting of protein–DNA association reactions. *Methods Enzymol.* 274, 478–492.
6. Petri, V. & Brenowitz, M. (1997). Quantitative nucleic acids footprinting: thermodynamic and kinetic approaches. *Curr. Opin. Biotechnol.* 8, 36–44.
7. Celander, D.C. & Cech, T.R. (1991). Visualizing the higher order folding of a catalytic RNA molecule. *Science* 251, 401–407.
8. Sclavi, B., Woodson, S., Sullivan, M., Chance, M.R. & Brenowitz, M. (1997). Time-resolved synchrotron X-ray 'footprinting', a new approach to the study of nucleic acid structure and function: application to protein–DNA interactions and RNA folding, *J. Mol. Biol.* 266, 144–159.
9. King, P.A., Jamison, E., Strahs, D., Anderson, V.E. & Brenowitz, M. (1993). 'Footprinting' of protein-DNA interactions using potassium peroxonitrite. *Nucl. Acids Res.* 21, 2473–2478.
10. Bai, Y. & Englander, S.W. (1996). Future directions in folding: the multi-state nature of protein structure. *Proteins.* 24, 145–151.
11. Celander, D.C. & Cech, T.R. (1990). Iron(II)-ethylenediaminetraacetic acid catalyzed cleavage of RNA and DNA oligonucleotides: similar reactivity toward single- and double-stranded forms. *Biochemistry* 29, 1355–1361.
12. Klassen, N.V. (1987). Primary Products in Radiation Chemistry. In *Radiation Chemistry Principles & Applications* (Farhatazis & Rodgers, M.A., eds.), pp. 29–61, VCH Publication. Texas, USA.
13. Hayes, J.J., Kam, L. & Tullius, T.D. (1990). Footprinting protein–DNA complexes with gamma-rays. *Methods Enzymol.* 186, 545–549.
14. Price, M.A. & Tullius, T.D. (1992). Using Hydroxyl radical to probe DNA structure. *Methods Enzymol.* 212, 194–219.
15. Franchet-Beuzit, J., Spotheim-Maurizot, M., Sabattier, R., Blazy-Baudras, B. & Charlier, M. (1993). Radiolytic footprinting. B rays, g photons and fast neutrons probe protein–DNA interactions. *Biochemistry* 32, 2104–2110.
16. Cech, T.R., Damberger, S.H. & Gutell, R.R. (1994). Representation of the secondary and tertiary structure of group I introns. *Nat. Struct. Biol.* 1, 273–280.
17. Michel, F. & Westhof E. (1990). Modeling of the three-dimensional architecture of group I catalytic introns based on comparative sequence analysis. *J. Mol. Biol.* 216, 585–610.
18. Cech, T.R. (1993). Structure and mechanism of the large catalytic RNAs: Group I and group II introns and ribonuclease P. In *The RNA World*, (Gesteland, R.F. & Atkins, J.F., eds.), pp. 239–269, Cold Spring Harbor Laboratory Press, New York, USA.
19. Cate, J.H., *et al*., & Doudna, J.A. (1996). Crystal structure of a group I ribozyme domain: principles of RNA packing. *Science* 273, 1678–1685.
20. Zarrinkar, P.P. & Williamson, J.R. (1994). Kinetic intermediates in RNA folding. *Science* 265, 918–924.
21. Murphy, F.L. & Cech, T.R. (1993). An independently folding domain of RNA tertiary structure within the *Tetrahymena* ribozyme. *Biochemistry* 32, 5291–5300.
22. Doudna, J.A., Cech, T.R. (1995). Self-assembly of a group I intron active site from its component tertiary structural domains. *RNA* 1, 36–45.
23. Lehnert, V., Jaeger, L., Michel, F. & Westhof, E. (1996). New loop–loop tertiary interactions in self-splicing introns of subgroup IC and ID: a complete 3D model of the *Tetrahymena thermophila* ribozyme. *Chem. Biol.* 3, 993–1009.
24. Heyduk, E. & Heyduk, T. (1994). Mapping protein domains involved in macromolecular interactions: a novel protein footprinting approach. *Biochemistry* 33, 9643–9650.
25. Burke, J.M., *et al*., & Tabak, H.F. (1987). Structural conventions for group I introns. *Nucleic Acids Res*. 15, 7217–7221.